PERGAMON

Deep-Sea Research II 46 (1999) 305–333

DEEP-SEA RESEARCH
PART II

Float trajectories in the deep western boundary current and deep equatorial jets of the tropical Atlantic

Philip L. Richardson*, David M. Fratantoni

Department of Physical Oceanography, Woods Hole Oceanographic Institution, Woods Hole, MA 02543, USA

Received 29 August 1997; received in revised form 19 March 1998

Abstract

Fourteen neutrally buoyant SOFAR floats at a nominal depth of 1800 m were tracked acoustically for 3.7 yr in the vicinity of the western boundary and the equator of the Atlantic Ocean. The trajectories revealed a swift, narrow, southward-flowing deep western boundary current (DWBC) extending from 7N across the equator. Two floats crossed the equator in the DWBC and went to 10S. Two other floats left the DWBC and drifted eastward in the equatorial band (3S–3N). Three floats entered the DWBC from the equatorial current system and drifted southward. These results suggest that at times the DWBC flows directly southward across the equator with a mean velocity of 8–9 cm/s averaged over long distances ($\sim$2800 km). At other times DWBC water is diverted eastward near the equator for long periods (2–3 yr), which can reduce the mean along-boundary velocity to 1–2 cm/s. This is much less than the instantaneous along-boundary velocities in the DWBC, which are often above 25 cm/s and occasionally exceed 50 cm/s. Mean eastward-flowing jets were observed near 2N and 2S bounding a mean westward jet centered on the equator (1S–1N). The southern jet at 2S coincides with a CFC-rich plume centered south of the equator. The CFC plume is inferred to have been advected by the southern jet across the Atlantic and into the Gulf of Guinea.

1. Introduction

This paper describes SOFAR float trajectories in the equatorial Atlantic at a nominal depth of 1800 m in North Atlantic Deep Water. The fundamental issue investigated is the exchange of water between the North and South Atlantic. Water-mass

* Corresponding author. Fax: 001 508 457 2181; e-mail: prichardson@whoi.edu.

0967-0645/99/$ – see front matter
PII: S0967-0645(98)00100-3

properties, such as chlorofluorocarbon (CFC) concentrations, imply that part of the deep western boundary current (DWBC) separates from the main current and flows eastward across the Atlantic near the equator and part continues southward along the western boundary. It is not known the extent to which the observed CFC plume lying near the equator and 1700 m (Weiss et al., 1989; Andrié et al., 1998) is due to advection or to enhanced mixing. Thus, a secondary issue investigated is the nature of the connection between the DWBC and flow along the equator.

The DWBC is the major pathway by which cold deep water flows southward across the equator into the South Atlantic and, eventually, into the Pacific and Indian Oceans (see Molinari et al., 1992; Friedrichs and Hall, 1993; McCartney, 1993, for descriptions of the DWBC in the tropical Atlantic based primarily on hydrographic data, and Fischer and Schott, 1997, for new current meter data). The warm upper layer in the Atlantic, including the Antarctic Intermediate Water, is thought to flow northward in compensation for the southward export of deep water. Schmitz and Richardson (1991) identified 13×10^6 m^3/s of upper level water from the South Atlantic flowing northward across the equator into the North Atlantic subtropical gyre and the Gulf Stream. This large-scale thermohaline circulation results in a northward heat flux through the Atlantic and is an important component of the world climate system (e.g., Broecker, 1991). An improved understanding of the thermohaline circulation and its variability is required in order to measure variations in the meridional flux of heat in the oceans and thus to infer variations in global climate.

The results described here are based on the continuation of an experiment begun in January 1989. An earlier technical report (Richardson et al., 1992) and two papers (Richardson and Schmitz, 1993; Richardson et al., 1994a) describe results from the first two years (21 months) of data. This paper (and a technical report by Richardson et al., 1994b) summarizes the entire 4 yr (44 months) of data (January 1989–September 1992), concentrating on data from the second 2 yr and the 1800 m float trajectories along the western boundary and equator. The float data are available through the WOCE subsurface float data assembly center in Woods Hole (http://wfdac.whoi.edu). The main new results are the long-term, 3.7 yr, float trajectories in the tropical Atlantic that reveal new information about the longer term fate and southward extension of the DWBC, which at times crosses the equator and at other times feeds into eastward equatorial currents. The floats also give a new Lagrangian view of the deep equatorial current system, its long time scales, and its connections to the currents along the western boundary.

2. Methods

During January and February 1989, 14 SOFAR floats were launched in the tropical Atlantic at 1800 m near the core of the upper North Atlantic Deep Water. The floats were tracked acoustically from January 1989 to September 1992 with an array of six moored autonomous listening stations (ALS; Fig. 1). Ten of the floats were launched along a line spanning the Atlantic between 6N and 11N, with closest spacing between floats near the western boundary off French Guiana, where the velocity is swiftest.

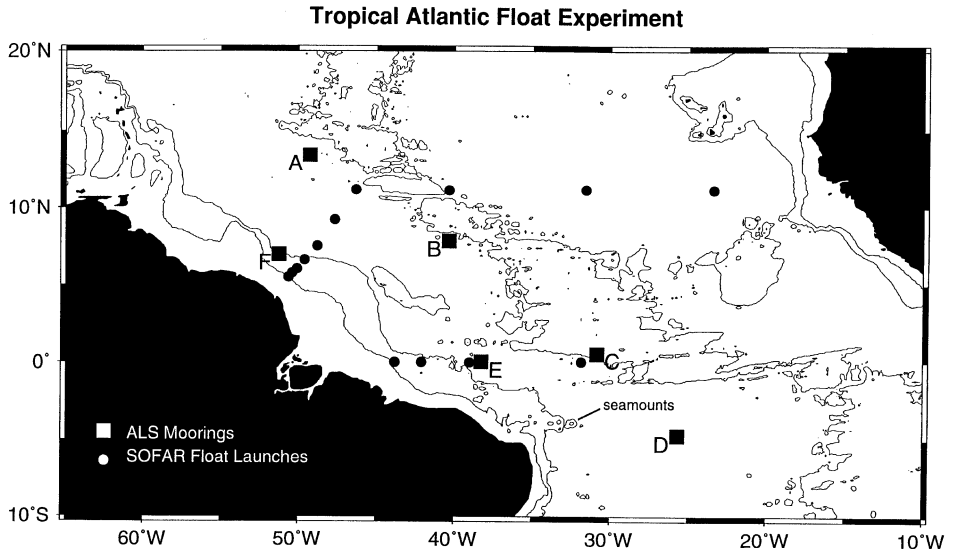

Fig. 1. Launch locations of 1800 m SOFAR floats (dots) in January and February 1989 and locations of Autonomous Listening Stations (squares) used to track the floats from January 1989 to September 1992. Depth contours, 2000 and 4000 m, are from Uchupi (1971). A line of seamounts near 4S is noted for later reference.

Four floats were launched along the equator in the west, where meridional flow is thought to cross the equator and eastward flow in the equatorial band originates. Thus the whole width of the Atlantic between French Guiana and West Africa was instrumented with floats, although sparsely in the eastern region (Fig. 1). Eight floats were heard to the end of the ALS records, a length of 44 months. Floats 2, 7, 8, 11, 12, and 15 died before the end of the 44 months. The mean lifetime of these six was 3.0 yr. A total of 40 float-years of trajectories were obtained by the 1800 m floats, roughly double the amount of data obtained during the first 21 months.

2.1. Temperature and pressure

The floats failed to transmit correct temperature and pressure data after launch, and they also failed to activate their buoyancy control, which would have kept them at constant pressure. Equilibrium depth at sea was estimated by following two floats acoustically from the ship as they sank and equilibrated at 1825 db (float 1) and 1775 db (float 6).

Without active ballasting, SOFAR floats gradually sink due to the slow deformation of their aluminum pressure housing. The sink rate was estimated to be 0.37 ± 0.05 db/d from ten historical floats that were found to give reliable long term estimates (see Richardson et al., 1992). This implies that the 1800 m floats would have sunk around 500–2300 m over the 44 months discussed here. The floats would have

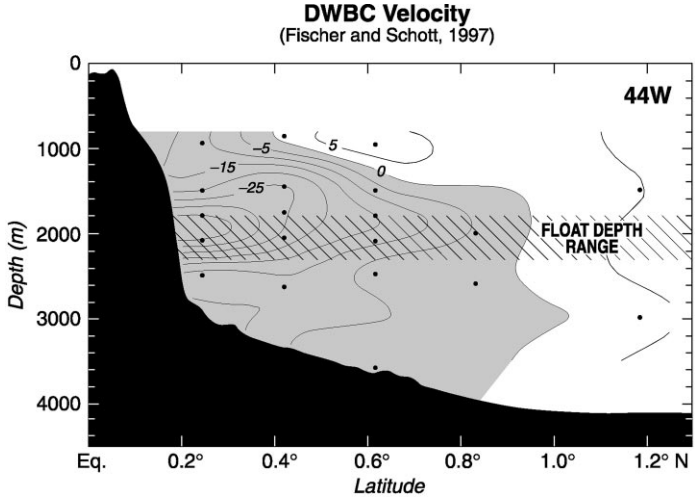

Fig. 2. Record length mean velocities (cm/s) in the DWBC near 44W as reported by Fischer and Schott (1997). Note that 44W intersects the western boundary near the equator. They found a peak daily velocity of 74 cm/s and a maximum record–mean velocity of 40 cm/s near a depth of 1800 m, adjacent to the boundary. The depth range of the nominal 1800 m floats which slowly descended to 2300 m by the end of the experiment is indicated by cross hatching.

remained within North Atlantic Deep Water although they would have descended below the high velocity region of the DWBC by the end of the experiment (Fig. 2).

2.2. Groundings

Three 1800 m floats on the inshore edge of the DWBC drifted into water shallower than their equilibrium depth and probably dragged along the sea floor. Float 10 clearly went aground after 51 d and remained stuck for the rest of the experiment. Float 6 was aground for 18 months near 3S. Float 8 was aground for four months and drifted southward very slowly ($\sim$1 cm/s) parallel to the topography from 5.0S to 6.5S. Charts differ considerably about the exact bathymetry, making it difficult to estimate depths of the grounded floats.

2.3. Float tracking and data processing

The floats transmitted an 80 s 250 Hz acoustic signal once per day. Float clock corrections and positions were calculated from the times of arrival of signals received at the moored listening stations. Spurious positions were edited manually, gaps less than 10 d long were linearly interpolated, and the resulting time series were smoothed by means of a Gaussian shaped filter (of weights 0.054, 0.245, 0.403, 0.245, and 0.054) to reduce position errors and tidal and inertial fluctuations. Velocity along trajectories was calculated at each final position by means of a cubic spline function.

The average error of a fix was estimated to be less than 10 km based on a comparison of float launch locations and first tracked positions.

3. DWBC trajectories

Summary plots of the trajectories, displacement vectors, and speeds of the 1800 m floats are given in Figs. 3–5. Clearly apparent are very long and fast trajectories along the western boundary and in the vicinity of the equator, especially compared to the very short and slow trajectory of float 7 in the northeast near 12N, 24W. The convoluted pattern of trajectories makes it difficult to see the large scale pattern of the flow along the western boundary. To clarify this pattern a schematic summary of float trajectories in the DWBC and near the equator was drawn (Fig. 6). In it the high-frequency and small-scale motions were subjectively removed, keeping what is interpreted to be the dominant low frequency and large scale motions. The continuity of the DWBC and its connection to zonal flow near the equator have been emphasized. For simplicity, eastward drifting portions of equatorial trajectories are shown

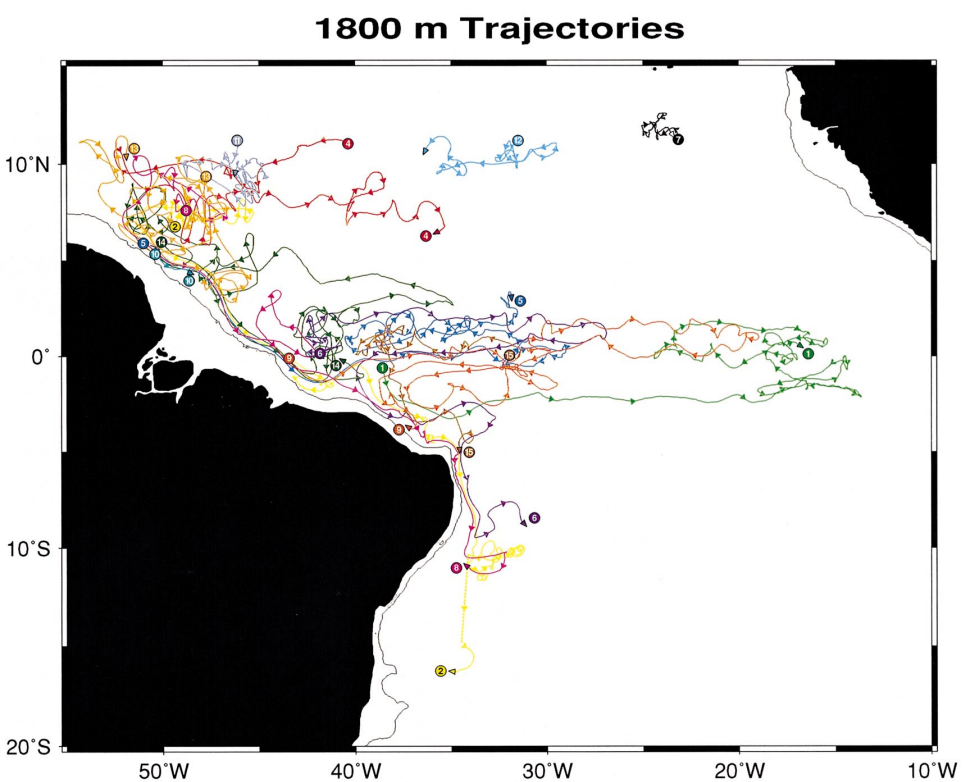

Fig. 3. Summary of 1800 m SOFAR float trajectories from January 1989 to September 1992. Arrowheads are spaced at intervals of 30 d along trajectories. Solid contour is 200 m (Uchupi, 1971).

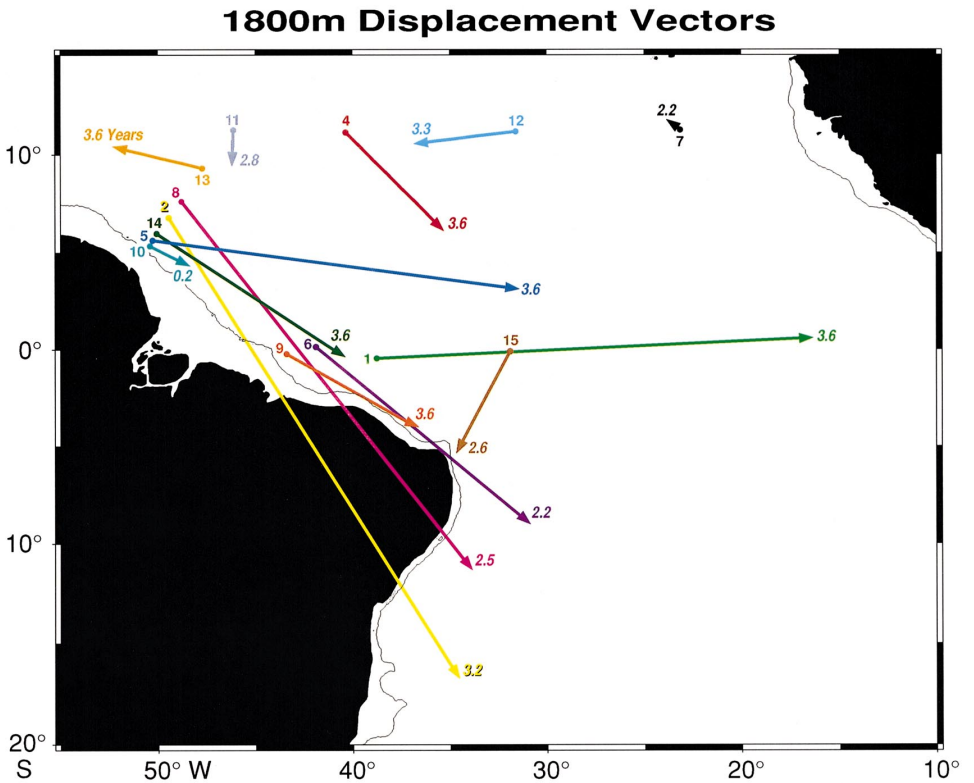

Fig. 4. Overall displacement vectors of 1800 m SOFAR floats. The number at the end of each vector is the duration of the trajectory in years. The duration for float 6 excludes the 1.5 yr it was aground and stuck near 3S, 38W. Solid contour is 200 m.

north of the equator and westward drifting portions south of the equator, although this is not meant to represent the actual meridional structure of the currents, which is more complicated than this as discussed later.

Five floats (2, 5, 8, 13, 14) were located in the DWBC near 7N. Two of these (2, 8) launched offshore of the DWBC drifted westward into the DWBC then southward across the equator reaching 16S and 11S (Figs. 3, 4 and 7). Both floats made small-scale (100–300 km) recirculations near the equator. Float 5 drifted southward in the DWBC until reaching the equator and then eastward to 29W, then back westward to 40W, and then eastward ending up near 3N 32W. Float 14 drifted southward in the DWBC to the equator, recirculated northward to 9N and drifted southward in the DWBC a second time, ending near 0N 40W.

The trajectory of float 13 is very convoluted, with portions in the DWBC and portions in recirculations some of which were located close to the western boundary. This trajectory, which ended near 10N 52W, was judged too complicated to include in the schematic. The trajectory of float 13 emphasizes the frequent exchanges between

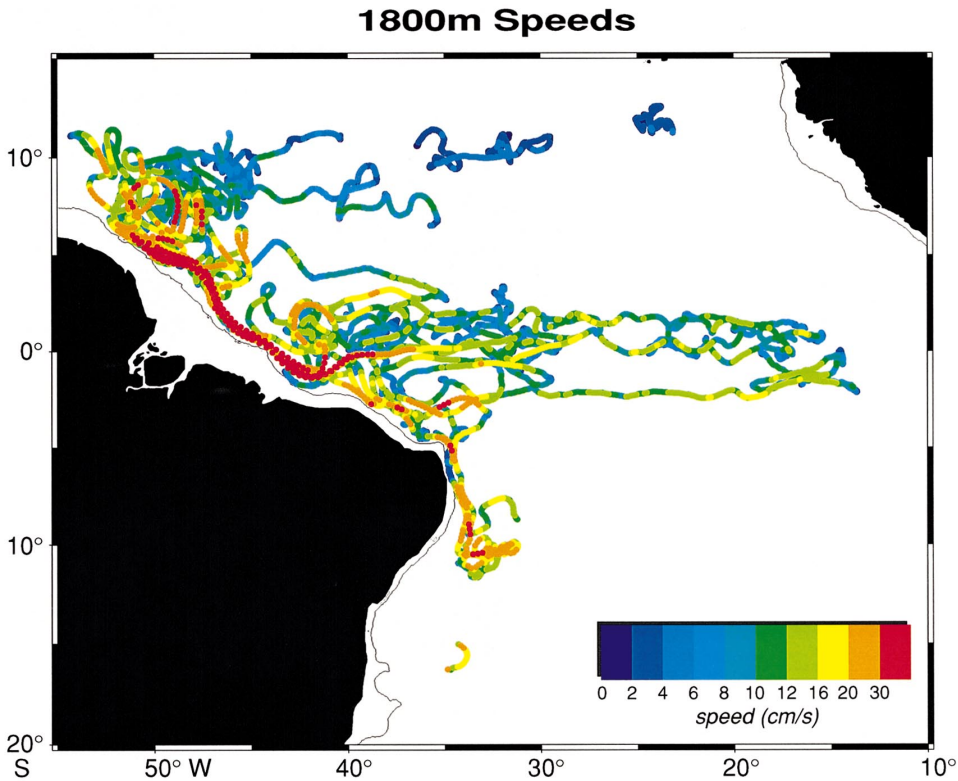

Fig. 5. Trajectories of floats color coded to reveal speed. Fastest speeds, reaching 55 cm/s, were measured along the western boundary near the equator (floats 5 and 14). Solid contour is 200 m. North of the equator the mean DWBC from floats was around 90 km wide.

the DWBC and recirculations. One possible explanation for why the trajectory of float 13 appears anomalous is that it was located below the high velocity core of the DWBC (see Fig. 2).

Almost all of the fastest velocities > 30 cm/s were observed in the vicinity of the western boundary (Fig. 5). Five floats (2, 5, 8, 10, 14) drifted fast southward paralleling the sea floor topography in the DWBC (Figs. 3 and 5). Four floats that either crossed 44W near the equator (2, 5, 14) or started there (9) measured peak speeds over 50 cm/s near 44W, and two (5, 14) reached 55 cm/s. The float velocities suggest that the DWBC increases in velocity as it flows down the boundary reaching a maximum velocity near 44W and the equator. This is consistent with the available moored current meter measurements in the same region (Johns et al., 1990, 1993; Schott et al., 1993; Colin et al., 1994; Fischer and Schott, 1997).

Fischer and Schott (1997) report that the dominant variability of the DWBC near 44W is a seasonal cycle or pulsing of the along-boundary currents with maximum velocity occurring in January and February. The fastest float velocities in the DWBC

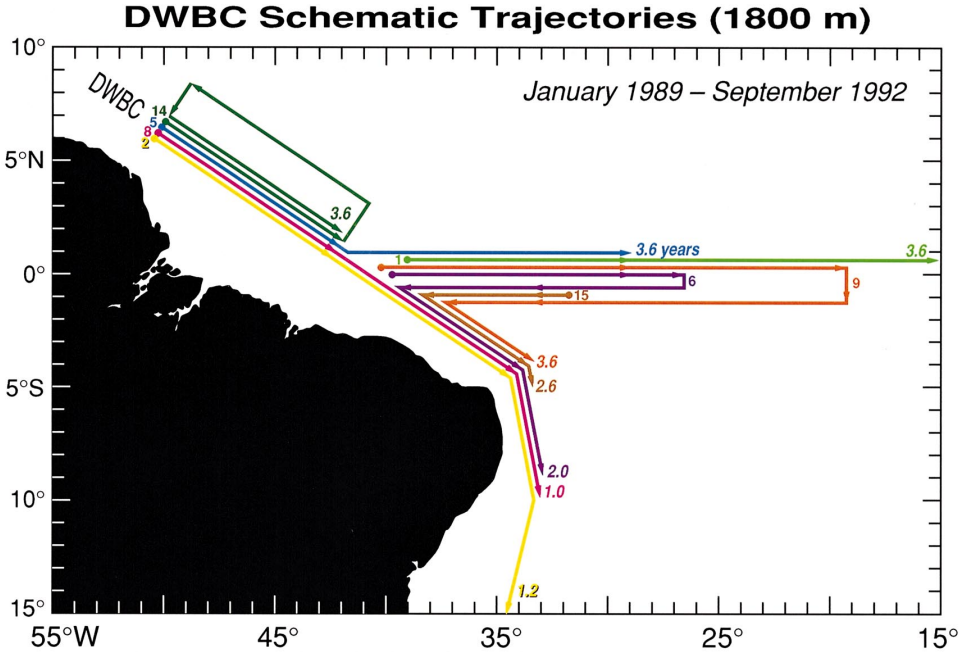

Fig. 6. Schematic diagram of 1800 m trajectories in the DWBC and near the equator. The trajectories were ordered in distance from the western boundary by how far south the floats traveled, starting with float 2 that went the farthest south. The numbers at the end of the trajectories are the duration in years from the float launch (floats 1, 5, 6, 9, 14 and 15) or when they started south in the DWBC (floats 2 and 8) to the end of the (schematic) trajectory. The value for float 6 excludes the 1.5 yr it was aground near 3S, 38W.

and the long along-boundary trajectories are centered at this time of year. The seasonal cycle provides an explanation of why some trajectories in the vicinity of the DWBC look more convoluted than others. The convoluted trajectories tend to occur when the along-boundary velocity is weak (centered in September and October). Five floats (2, 4, 8, 13, 14) looped and meandered just offshore of the western boundary, illustrating that at times there is no continuous along-boundary flow. The fastest speeds in these loops and meanders tend to be found in two regions. The first is near 4N–11N where the North Brazil Current retroflects and sheds rings that translate northwestward up the coast (Johns et al., 1990; Didden and Schott, 1993; Richardson et al., 1994a; Fratantoni et al., 1995). A maximum of velocity in the North Brazil Current and in its ring shedding occurs in September–October when the DWBC is near its minimum. It is possible that a deep extension of the retroflection and rings could have influenced the motions of these floats and caused a temporary disruption of the along-boundary current. The northwestward flow on the inshore part of the anticyclonic (clockwise) rings is counter to the mean southeastward flow in the DWBC. The swirl velocity of the rings extended deeper than 900 m where looping floats in rings measured a swirl velocity of 35 cm/s (Richardson et al., 1994a, see also

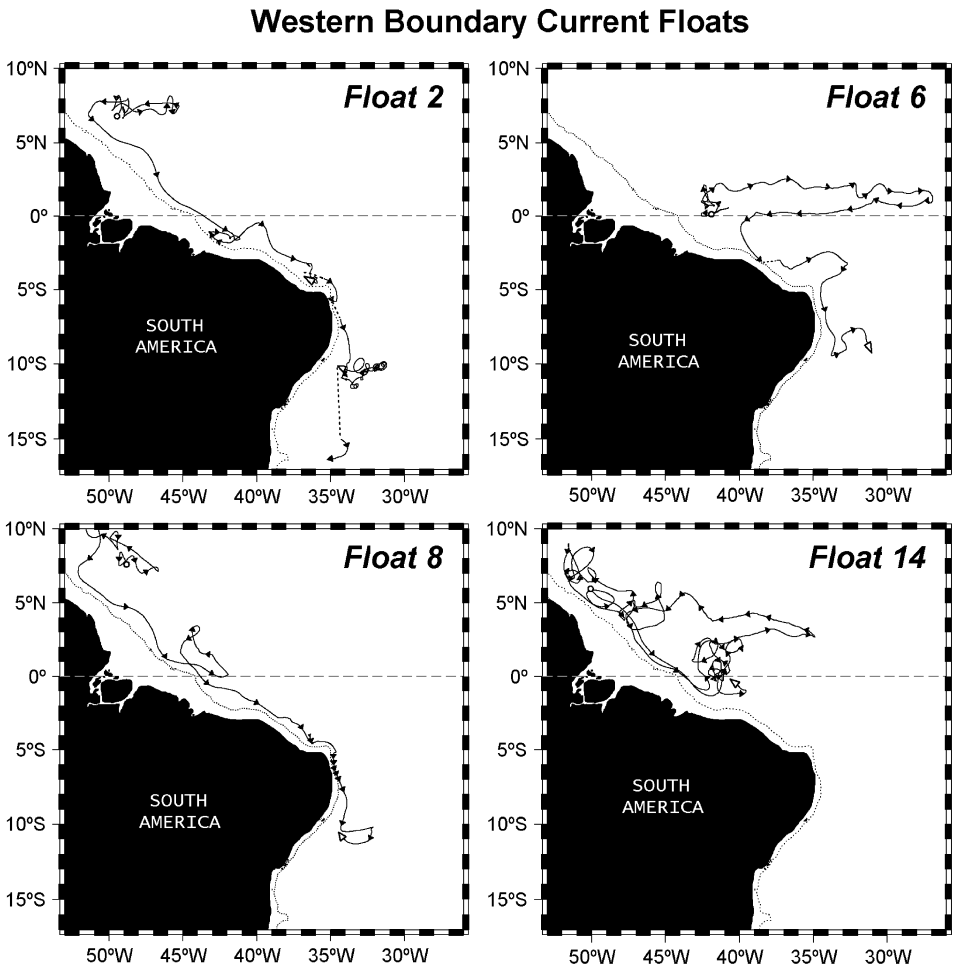

Fig. 7. Examples of individual 1800 m float trajectories along the western boundary. The depth contour is 200 m. Arrowheads are spaced at 30-d intervals. Floats 2 and 8 were entrained into the DWBC in January 1990 (float 5) and March 1990 (float 2). Float 2 drifted the farthest south; the gap between 12S and 15S was caused by topographic blocking of the acoustic signals as the float (probably) drifted closer to shore and back out again. Float 6 was launched near the equator in January 1989. It entered the DWBC in September 1990, grounded in October 1990, and continued southward beginning in April 1992. Float 14 drifted southward in the DWBC to the equator, recirculated northward to 9N and drifted southward in the DWBC a second time ending near 0N 40W.

Fratantoni et al., 1995). Some high speed portions of the 1800 m trajectories (Figs. 3 and 5) look like they could have been below rings.

The second region of high velocity is located near 10S 33W where float 2 (and 8) looped in a coherent cyclonic eddy for 170 d (Fig. 8). This is the only coherent eddy observed by 1800 m floats as documented by more than two consecutive float loops.

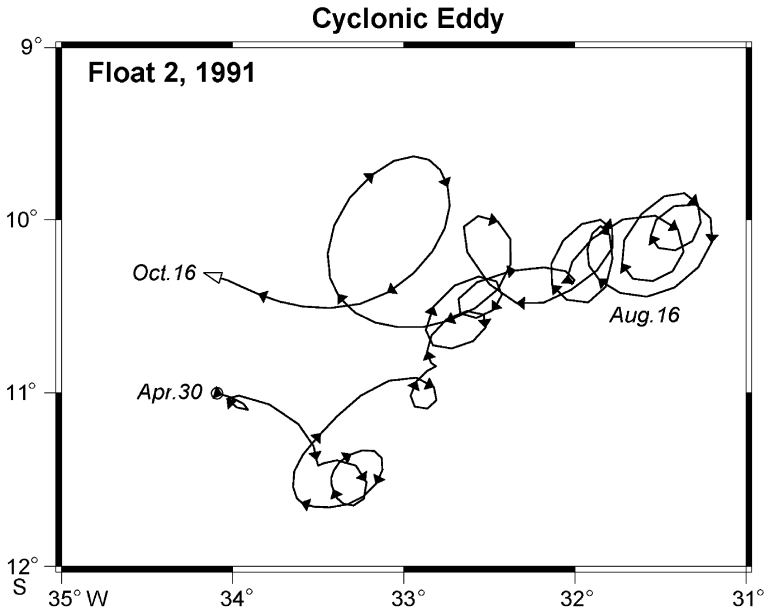

Fig. 8. Trajectory of float 2 while it was looping in a cyclonic (clockwise) eddy from April to October 1991. The float looped 15.5 times with a period of 11 days and a swirl velocity of 16 cm/s. Arrowheads are spaced at 5-d intervals.

The eddy did not translate very far during the nearly six months it was observed. The presence of energetic cyclonic eddies in this second region is further documented by a 2500 m float that looped near 5S–10S, 31W–34W for nearly 18 months during 1993 and 1994 (Hogg and Owens, 1998). These eddies are probably pieces (offshore meanders, extrusions) of the DWBC that have separated from the boundary.

3.1. DWBC velocity

A mean velocity profile across the DWBC and its recirculation was calculated by converting float positions to distances seaward of the 1800 m depth contour and by rotating velocity components to be normal and parallel to the contour (Fig. 9). The mean velocity, eddy kinetic energy (EKE), and transport per unit depth were calculated in 10-km-wide bins parallel to the 1800 m contour. Floats east of 43W south of 3N were omitted from the composite to screen out those in swift equatorial currents. Fig. 9 is thus both a space (11N–1S) and time (44 month) average, which shows the mean structure of the DWBC along the western boundary.

The mean DWBC is 90 km wide, reaches a peak mean velocity of 20.8 cm/s (at 45 km), and has an integrated transport (per unit depth) of 10.8×10^3 m^2/s. Both the peak velocity and the transport are smaller than the values of 26 cm/s, 13.8×10^3 m^2/s determined from the first two years of trajectory data (Richardson and Schmitz, 1993). This is probably due to the floats having descended below the high velocity core of the

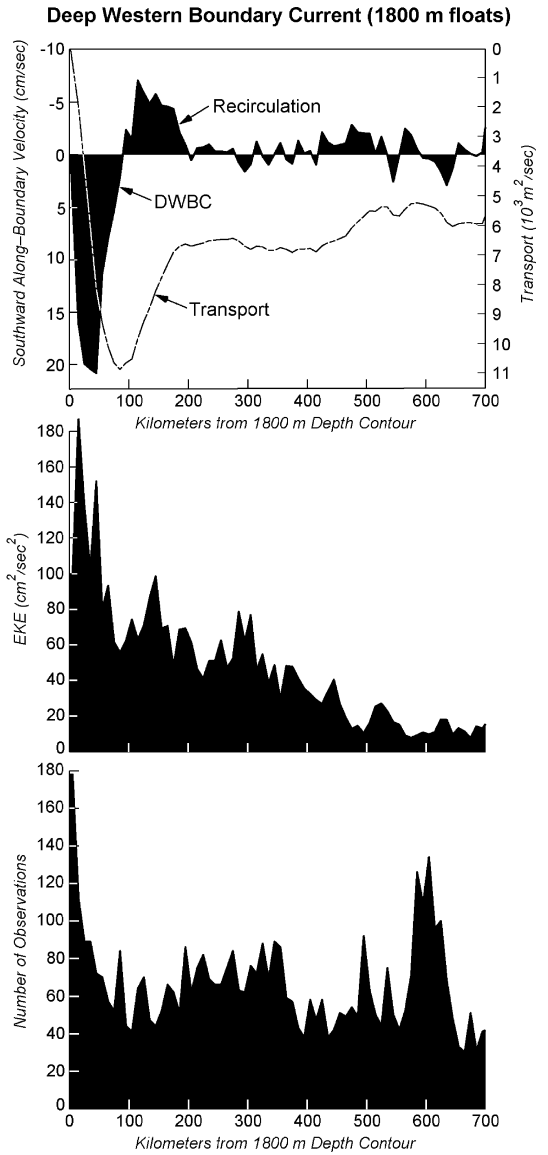

Fig. 9. Average along-boundary velocity, transport, and eddy kinetic energy and number of observations at 1800 m (nominal) in the vicinity of the DWBC west of 43W. All available individual daily velocities were grouped and averaged in 10-km wide bins parallel to the 1800 m depth contour which was obtained using ETOPO2 data. Nine different floats were used in this composite which consists of 4663 daily velocity observations. Seven floats drifted in the region of the DWBC jet and provided 803 daily observations. The figure was terminated at 700 km because much sparser numbers of observations are located seaward of this point. Transport per unit depth (m^2/s) was obtained by summing in the seaward direction the product of bin width and the average velocity in each bin. Eddy kinetic energy was calculated using $1/2(\overline{u'u'} + \overline{v'v'})$ where $\overline{u'u'}$ and $\overline{v'v'}$ are the variances of the velocity values about the mean velocities, $\bar{u}$ and $\bar{v}$ where $u' = u - \bar{u}$ and $v' = v - \bar{v}$. This is an update of Fig. 6 shown by Richardson and Schmitz (1993), including the newer data.

DWBC during the last 2 yr of the experiment. Fig. 9 includes data from float 13 which seems less like the other DWBC floats that drifted fast southeastward along the boundary. The peak mean velocity in the DWBC is less than that measured by Fischer and Schott (1997) near 44W because the floats averaged over a much larger region than did the current meters.

The swift DWBC jet coincides with a high EKE band $> 100\,\mathrm{cm^2/s^2}$. Offshore of this EKE gradually decreases to around $10\,\mathrm{cm^2/s}$ near 700 km.

3.2. Recirculation north of the equator

Offshore of the DWBC, between 90 and 200 km, is a narrow ~ 110 km wide recirculation region (Fig. 9). The northward along-boundary velocity peaks at 6.9 cm/s and the mean velocity in the narrow recirculation region is 3.8 ± 0.3 cm/s where the standard error was estimated using the eleven average velocities in the 10-km wide bins. The transport per unit depth integrated over the 90–200 km band is $4.2\ (\pm 0.3) \times 10^3\ \mathrm{m^2/s}$ and over the larger region 90 km to 700 km is $4.9\ (\pm 0.8) \times 10^3\ \mathrm{m^2/s}$. The net southward transport per unit depth integrated from the 1800 m contour out to 700 km is $5.9 \times 10^3\ \mathrm{m^2/s}$. This implies that 39% of the DWBC at the depths of the floats recirculated within a distance of 110 km of the DWBC and that 45% recirculated within 610 km of the DWBC. The new net southward transport of $5.9 \times 10^3\ \mathrm{m^2/s}$ within 700 km of the boundary is smaller than the $9.8 \times 10^3\ \mathrm{m^2/s}$ calculated for the first two years. The difference is due to both the reduced transport of the DWBC and an increase from 4.0×10^3 to $4.9 \times 10^3\ \mathrm{m^2/s}$ of the recirculation transport. The main increase in recirculation transport appears to be located in the 90–200 km band just offshore of the DWBC where float 14 recirculated. The size of the recirculation transport and the net transport appears to depend strongly on the characteristics of the relatively few float trajectories. The uncertainty of values depends on how well the float trajectories sampled the recirculation which appears to vary with distance offshore and presumably in time like the DWBC (Fischer and Schott, 1997; Gouriou et al., submitted).

3.3. DWBC crosses the equator

There is good evidence that most of the DWBC water at the depths sampled by floats crosses the equator in the west either directly (floats 2 and 8) or indirectly after being recirculated (float 14) or after an eastward diversion in the equatorial jets. Floats 1, 5 and 9 show a direct connection between flow in the DWBC north of the equator and eastward flow near the equator. Floats 6, 9 and 15 show that water near the equator can eventually return to the western boundary and go south in the DWBC. Taken together, the above two groups of floats imply that DWBC water can go eastward in the equatorial band but that the water probably eventually returns westward and continues southward in the DWBC. A possible explanation for why floats 1 and 5 never returned to the western boundary is that by the latter part of the experiment they had descended below 2200 m where the zonal equatorial currents are weaker (see Ponte et al., 1990; Fischer and Schott, 1997; Gouriou et al., submitted).

Floats 2 and 8 took 14 months and 12 months to go from 7N to 10S, with record-length mean along-boundary velocities of 8.1 and 8.6 cm/s, respectively. If we include the time required for the floats to drift from their launch locations into the DWBC, then the record-length mean along-boundary velocity decreases to 4.0 cm/s for both floats. The velocity estimate for float 8 was adjusted for the 4.3 months it was aground and slowly (1.5 cm/s) dragging along the sea floor. The mean along-boundary velocity of float 14, including its two passes down the boundary from roughly 6N to the equator and its recirculation, was 1.1 cm/s. The mean along-boundary velocities of floats 6 and 9 from their launch locations near the equator to 9S (float 6) and 4S (float 9) were 2.2 and 0.7 cm/s, respectively. The value for float 6 was adjusted for the 18 months it was aground near 3S. The apparent mean velocity of the DWBC has been estimated from tracers to be around 1 cm/s (Weiss et al., 1985, 1989; Doney and Jenkins, 1994). Because of the way tracers in the DWBC mix with nearby water and the assumptions used to estimate the mean velocity, the 1 cm/s value could be biased low by as much as a factor of 5 (Pickart et al., 1989; McCartney, 1993; Doney and Jenkins, 1994; Rhein, 1994). The mean velocity of CFC in the DWBC could therefore be 1–5 cm/s, a range in accord with the mean velocity from floats as described above.

The three DWBC floats (2, 6 and 8) that went the farthest south diverged away from the western boundary south of 8S where the boundary becomes more southwestward. Float 2 left the boundary and became trapped in a cyclonic eddy near 10S 32W for 170 d (Fig. 8). After leaving the eddy float 2 continued southward to 16S although tracking was intermittent because topography blocked the acoustic signals. Float 8 drifted south to 10.5S and made a partial cyclonic loop around the eddy in which float 2 was trapped. Float 6 went south to 9.5S then turned and drifted eastward. Four recent WOCE floats launched near the western boundary at 7S–13S at a depth of 2500 m drifted south (two went to 23S), providing information about the downstream continuation of the DWBC (Hogg and Owens, 1998).

4. Equatorial trajectories

Four floats (1, 6, 9 and 15) were launched near the equator in the western Atlantic. Float 1 drifted eastward along 2S ending up in the eastern Atlantic near the equator (Fig. 10). Float 6 went eastward along 2N to 27W, returned westward along 0N–1N, then entered the DWBC and went southward past 9S (Figure 7). Float 9, launched in the DWBC on the equator, drifted eastward to 30W near the equator, then up to 2N and farther eastward to 19W, then back westward along the equator to the western boundary, and southward to 4S. Float 15 drifted slowly westward along the equator, then southward along the western boundary, ending at 5S.

4.1. Zonal jets

The four floats launched near the equator plus two others (5 and 14) that drifted south to the equator in the DWBC reveal swift zonal currents in the equatorial band 3S–3N. Once in this band the floats tended to stay there, drifting long distances

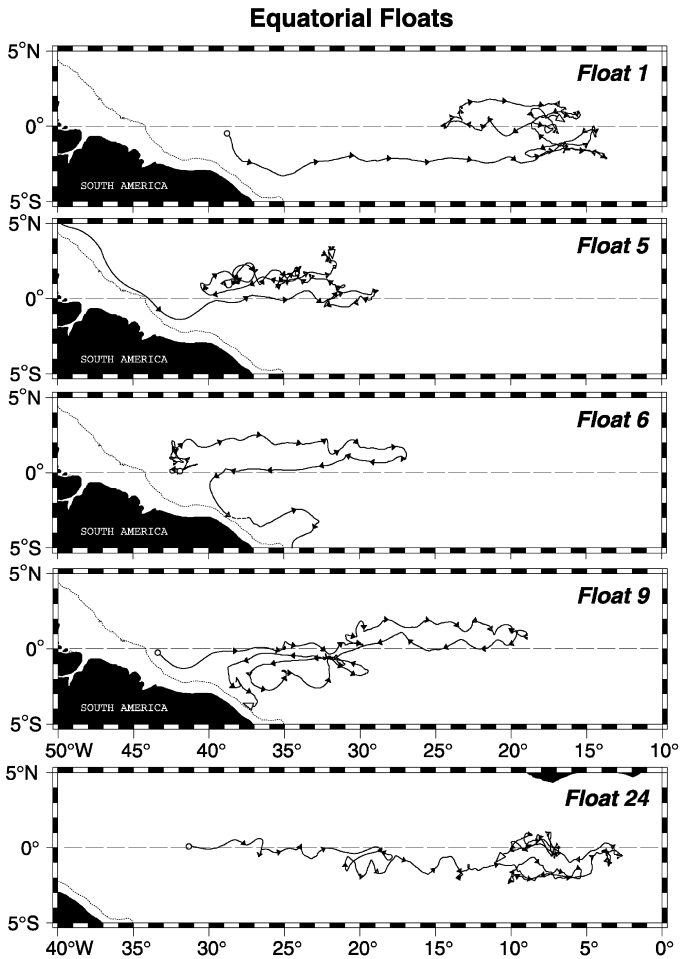

Fig. 10. Examples of individual 1800 m float trajectories near the equator. The depth contour is 200 m. Arrowheads are spaced at 30-d intervals. Floats 5 and 9 in the DWBC entered the equatorial band and went eastward. Float 9 returned west and re-entered the DWBC south of the equator at the end of the tracking. Float 6 which was in the equatorial currents entered the DWBC south of the equator. Float 24, ballasted to lie within an eastward equatorial jet, equilibrated near 1125 m. This float is shown here because it also drifted eastward in the vicinity of the southern jet.

zonally, except in the west where a direct connection to meridional flows along the boundary was observed.

These six floats provide evidence for mean eastward flowing jets centered at 2N and 2S bounding a mean westward jet near the equator. For simplicity the two eastward jets will be referred to as the northern and southern jets. The jets are apparent in individual float trajectories (Fig. 11) and in a summary figure (Fig. 12) that shows mean zonal velocities east of 40W. A peak mean eastward velocity of 9.9 ± 3.1 cm/s

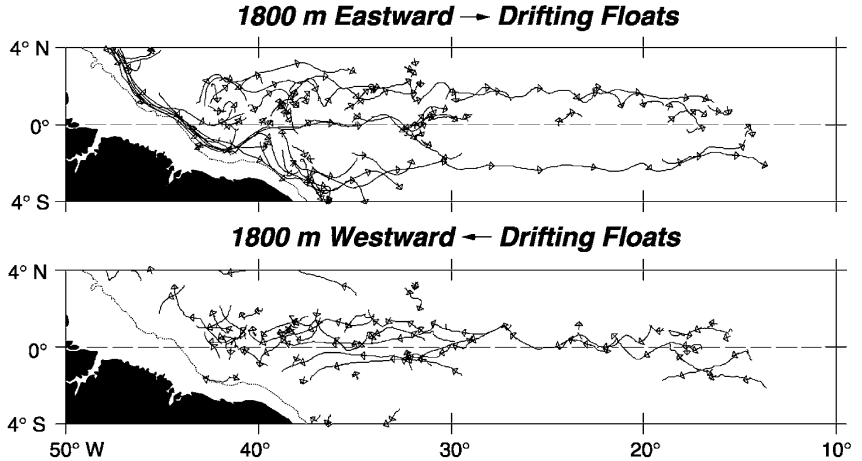

Fig. 11. Near equatorial trajectories subdivided into eastward and westward drifting portions. Trajectories reveal eastward currents centered near 2N and 2S and westward currents centered near the equator except for some eastward flow near the equator in the western region during the first six months of the experiment.

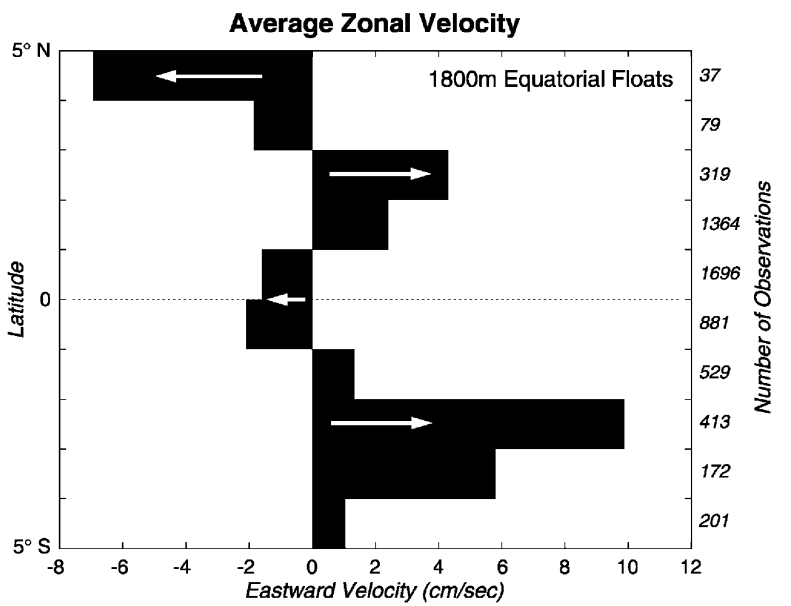

Fig. 12. Mean eastward velocity of the near equatorial floats in 1° latitude bins east of 40W. The general pattern is eastward equatorial jets centered near 2N and 2S with a mean westward jet centered on the equator, 1S–1N. Float 14 located north of 3N recirculated northwestward causing the westward velocities there. The number of daily velocity observations in each band is listed near the right-hand edge. The standard error of the mean velocities between 3N and 3S is estimated to be $\pm$ 2.6 cm/s.

was centered at 2.5S in the southern jet and 4.3 ± 3.3 cm/s at 2.5N in the northern jet. These eastward jets bound westward velocity of around 1.8 cm/s near the equator.

4.1.1. Northern jet

The evidence for the northern jet consists of five different floats (1, 5, 6, 9 and 14) that drifted eastward near 2N at various times from July 1989 to May 1992 (Table 1). If we assume that the floats were all in the same jet, then its thickness would be at least 400–500 m, the depth range sampled by the gradually sinking floats during the experiment. A crude estimate of transport in the northern jet is 3×10^6 m^3/s based on a two-degree latitude width, a 500 m thickness, and a mean velocity of 2.8 ± 1.2 cm/s between 1N and 3N (see Table 2). The mean velocity of the five floats mentioned above is 4.6 ± 1.1 cm/s.

4.1.2. Southern jet

The best evidence for the southern jet is given by float 1, which translated from the western boundary near 39W eastward to 14W along 2S during February to November 1989 (Table 1). One other float provides supplemental evidence for a persistent jet near 2S. Float 24, which equilibrated at 1125 m and is inferred to have gradually descended to around 1600 m by the end of the experiment, drifted eastward near 1S–2S from 21W to 6W between September 1989 and June 1990. If we assume that floats 1 and 24 were both located in the same eastward jet, then it was at least 700 m thick and continuous from the western boundary into the Gulf of Guinea. The mean eastward velocity from float 24 in the 1S–3S band is 4.1 ± 2.7 cm/s, somewhat slower than the 5.7 ± 3.7 cm/s observed by float 1 (Table 2). The average velocity of the 1800 m floats plus float 24 in the band 1S–3S is 4.9 ± 1.9 cm/s. At this rate a float that remained in the 2S jet would translate across the Atlantic to 4W in around 2.6 yr. The implied transport of the southern jet is around 8×10^6 m^3/s based on a two-degree width, 700 m thickness and 4.9 cm/s mean velocity.

Table 1
Eastward drifting floats in the equatorial jets

Float	Dates	Longitudes (W)
Northern jet (3N–1N)		
1	September 91–May 92	24 → 15
5	January 91–March 92	40 → 32
6	July 89–March 90	42 → 27
9	October 89–May 90	30 → 19
14	August 89–January 90	42 → 35
Southern jet (1S–3S)		
1	February 89–November 89	39 → 14
6	April 92–May 92	38 → 33
9	June 91–September 91	37 → 32
15	May 91–June 91	37 → 34
24	September 89–June 90	21 → 6

Table 2
Velocity of zonal jets

Lat	$\bar{u}$ (cm/s)	Number of observations	N/τ	$\overline{u'u'}$ (cm^2/s^2)	Comments
Method 1					
3N–1N	2.8 ± 1.2	1683	44	32	Northern jet
1N–1S	-1.8 ± 1.3	2577	62	49	Equatorial jet
1S–3S	5.1 ± 2.2	942	27	66	Southern jet
1S–3S	4.9 ± 1.9	1168	34	59	Including float 24
Method 2					
3N–1N	4.6 ± 1.1	5		4.6	Floats 1, 5, 6, 9, 14
1S–3S	4.1 ± 0.9	3		1.8	Floats 1, 9, 24
Selected individual floats					
3N–1N	5.4 ± 3.0	179	5	23	Float 1
3N–1N	0.5 ± 1.7	736	16	24	Float 5
3N–1N	6.6 ± 3.3	238	6	32	Float 6
3N–1N	5.8 ± 2.6	241	6	20	Float 9
3N–1N	4.4 ± 5.8	86	3	51	Float 14
1S–3S	5.7 ± 3.7	468	11	75	Float 1
1S–3S	2.5 ± 2.9	330	9	38	Float 9
1S–3S	4.1 ± 2.7	226	7	26	Float 24

Statistics for groups of floats were calculated by two methods. In the first method all individual float daily velocity values were grouped into bands 2° in latitude, east of 40W, and average velocity, variance, and N/τ calculated. Standard error of velocity was estimated using $[2\overline{u'u'}/(N/\tau)]^{1/2}$ where $\overline{u'u'}$ is the variance about the mean velocity $\bar{u}$, and N/τ is the sum of the number of 50-d intervals each float was within a band. The 50 d is an estimate of the integral time scale τ of the Lagrangian autocorrelation function. In the second method selected floats were considered to give an independent estimate of mean velocity in each jet. Mean velocities from different floats in each band were then grouped and averaged. Standard error of velocity was estimated using $\sqrt{\overline{u'u'}/(n-1)}$ where n is the number of mean velocity values in each band, five for 3N–1N and three for 1S–3S. In the 1S–3S band only the three floats (1, 9 and 24) which measured the largest numbers of daily velocities were used. In the 3N–1N band the first method gives a smaller mean velocity because of the large number (736) of daily observations of float 5 which had a small 0.5 cm/s mean velocity and because the mean included float 15 which was not included in method 2 (because float 15 only occasionally extended into the 3N–1N band and did not look like it was representative of the northern jet).

Evidence from a few additional floats suggests that the southern jet extended from 800 m down to 2500 m. During 1989–1992 two 800 m floats (Richardson et al., 1994) drifted eastward in the 1S–3S band with a mean zonal velocity of 7.7 ± 2.6 cm/s (391 daily observations). More recently in 1994 and 1997 some French floats drifted eastward between 1S asnd 3S, providing evidence of a long-term mean eastward velocity there (Ollitrault, 1998). A long eastward drift of a 2500 m RAFOS float near 2S was measured by Hogg and Owens (1998). This float (203) drifted from 36W to 19W between April 1994 and August 1995 with a mean velocity of 4.4 ± 2.4 cm/s in the 1S–3S band. If the thickness of the southern jet was at least 1700 m as implied by these additional trajectories then its transport estimated by grouping all available

800–2500 m floats (2658 daily observations) in the 1S–3S band and calculating the average velocity (4.2 ± 1.2 cm/s) could be at least 16×10^6 m^3/s.

Fischer and Schott (1997) found that near the eastern tip of Brazil (35W) the DWBC splits into two cores, a weak one attached to the boundary and the main one flowing eastward between 2S and 3S along the northern side of a line of seamounts located along the Fernando de Noronha Ridge near 4S (Fig. 1). A maximum in CFC concentration coincided with the main core between 2S and 3S (Rhein et al., 1995). The float trajectories agree with these results and add information about where the water goes downstream of 35W. Two floats (2 and 8) drifted southeastward rather slowly along the western boundary, in agreement with Fischer and Schott's (1997) speculation that the weaker core might be due to leakage through gaps in the seamount chain farther upstream. Four floats drifted eastward in the main jet near 2.5S 35W (Table 1). Float 9 recirculated northward to the equator, then westward, and then southward near the boundary. Float 1 continued a long way eastward into the eastern Atlantic. Floats 6 and 15 turned south after crossing 35W merging with the trajectories of floats 2 and 8, which had drifted along the boundary. These few trajectories suggest that part of the water in the southern jet at 35W continues eastward and part continues southward.

None of the five floats that crossed 44W in the very swift DWBC (see Fig. 2) directly entered the southern jet near 35W. Floats 2 and 8 continued southeastward from 44W along the boundary, floats 5 and 9 drifted eastward near the equator, and float 14 recirculated northwestward. Of the four floats that drifted eastward in the southern jet near 35W floats 6, 9 and 15 had all spent time in the equatorial band east of the DWBC. All three eventually drifted westward near the equator before entering the southern jet. Only float 1 drifted from its launch location near 0N 39W directly southeastward into the jet. The trajectories suggest that the pathways between the swift DWBC near the equator and the southern jet are complex and highly variable.

4.1.3. Equatorial jet (1S–1N)

The evidence from 1800 m floats is for eastward flow near the equator 1S–1N from the western boundary to 30W during February–July 1989 (floats 5 and 9), followed by predominantly westward flow for the rest of the experiment (floats 1, 5, 6, 9, 15). The experiment–mean velocity in the 1S–1N band is westward at 1.8 ± 1.3 cm/s. If we exclude the first six months of eastward velocities (floats 5 and 9), the mean velocity nearly doubles to 3.4 cm/s westward.

The new data presented here support results from vertical profiles of velocity (Ponte et al. 1990; Rhein et al., 1995; Fischer and Schott, 1997; Gouriou et al., submitted) and current meter records (Fischer and Schott, 1997), which indicate that the flow on the equator consists of a series of vertically stacked zonal jets alternating in direction. The jets appear to have long period (several year) variations as observed by current meters near 35W. During most of the experiment the velocity at the float depth was westward, which carried floats 6, 9 and 15 westward into the DWBC. The change from eastward to westward velocity observed by the near-equatorial floats (1S–1N) could have been partly caused by their gradual sinking from an eastward jet into a westward one. Therefore the mean westward velocity should be interpreted as being

a combination of both temporal (over 3.7 yr) and vertical (over 500 m) variations of the equatorial currents.

4.1.4. Exchanges between jets

Although there is evidence for mean eastward flow across the Atlantic in the eastward jets, individual floats left the jets before going all the way across. Within the equatorial band of 3S–3N the floats moved meridionally from one jet to another and switched directions. For example floats 1, 9, and 24 left the southern jet and entered the equatorial jet, floats 1, 5 and 9 left the equatorial jet and entered the northern jet, and floats 5, 6 and 9 left the northern jet and entered the equatorial jet. None left the 3S–3N band except in the west.

Some trajectories suggest that the mid-Atlantic Ridge caused a disruption or partial blocking of the zonal flows and enhanced the exchange between jets. Float 5 ceased its rapid eastward translation along the equator at the Ridge crest, float 6 reversed direction near the Ridge, float 9 switched from the equator to the northern jet near the Ridge crest, and float 1 ceased its long and fast eastward translation in the southern jet over the Ridge and began a complicated series of eastward and westward zonal fluctuations. Although complicated, the trajectory of float 1 near the Ridge is generally consistent with the meridional distribution of zonal jets as shown in Fig. 12.

4.1.5. Seasonal variation of the jets

A time series of monthly mean eastward velocity in each jet is shown in Fig. 13. The best evidence of a seasonal cycle is in the northern jet where eastward velocity reaches 6.4 cm/s in December and westward velocity is 0.5 cm/s in July. Considering the size of the estimated standard error ~ 2 cm/s of the monthly mean, the evidence for reversal in direction in June and July is poor. The range of the seasonal variation 6.9 cm/s is large compared to the mean velocity of 2.8 ± 1.2 cm/s (Table 2).

A rather similar annual cycle is observed in the equatorial jet when the first six months of eastward velocity are excluded. A maximum westward velocity of 5.7 cm/s occurs in July and a minimum westward velocity of 0.7 cm/s is in January. The 5.0 cm/s range of the seasonal velocity is roughly similar to that of the northern jet, and the phases of the two series agree well – maximum eastward velocity anomalies (from the mean) occur in November–January, maximum westward anomalies in June and July. Therefore much like the DWBC at 44W the northern and equatorial jets appear to pulse seasonally. The maximum eastward velocities in the northern jet lead the maximum southeastward transport in the DWBC at 44W by about 1.5 months.

The evidence of seasonal variation of the southern jet is poorer than for the other two jets. The main floats in the southern jet (floats 1, 9 and 24) do not appear to drift faster in November–January as several floats in the northern jet did. Float 1 continued fast eastward from February to October 1989 as did float 24 from October 1989 to July 1990 and float 9 from June to August 1991 (with some higher frequency fluctuations superimposed). Because of the low number of floats in the southern jet, one long trajectory like that of float 1 had a large effect on the time series. Based on the time series (Fig. 13) the range of velocity is 2.0 cm/s and maximum eastward velocity

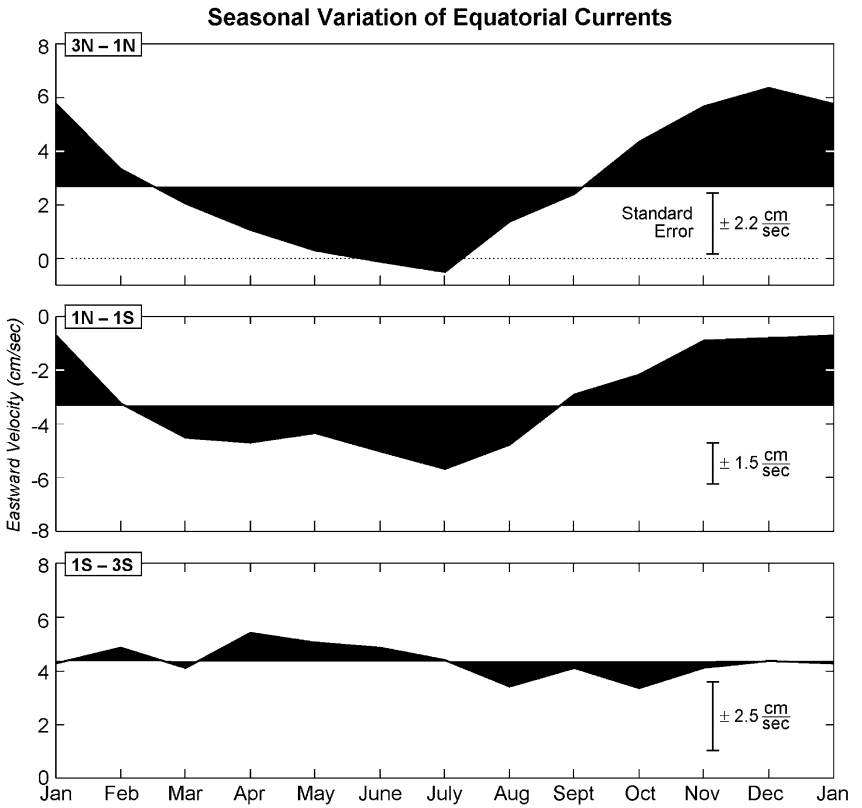

Fig. 13. Seasonal variation of eastward velocity in three bands 3N–1N, 1N–1S, and 1S–3S, east of 40W. Individual velocities were grouped into monthly bins (including all years) and averaged. The series were smoothed lightly with a three-month top hat filter to reduce some month-to-month jitter. The first six months of data in the 1N–1S band were omitted to eliminate the swift eastward jet measured by floats 5 and 9 during that period. Estimates of standard errors are added.

occurs in March. The range is much less than that of the other two jets, and the phase does not match the other two.

A seasonal cycle of zonal currents also has been observed in two-year-long current meter records (1700–3950 m) in the vicinity of the equator (Thierry et al., 1998). At both 0.7N 14.8W in the Romanche Fracture Zone and 0.9S 13.5W in the Chain Fracture Zone the zonal velocity at a depth of 1700 m had a dominant annual harmonic within amplitude around 10 cm/s. Maximum eastward velocity occurred in November–December. The phase agrees well with the float observations but the amplitude is about two times larger. Thierry et al. (1998) explained the current variations as being due to long Rossby waves with periods of 12 months and 6 months; baroclinic mode 3 and meridional mode 3 were dominant. These results and those of Hall et al. (1997) near 36W show that throughout the deep

equatorial region the various current regimes pulse seasonally as do the near surface currents.

The annual period oscillations of deep zonal currents near the equator also have been observed in many numerical models (see, for example, Böning and Schott, 1993). These current oscillations have the characteristics of long Rossby waves and are thought to be a deep baroclinic response to the seasonal cycle of wind forcing over the equatorial Atlantic.

4.1.6. Waves

As the floats drifted zonally in the equatorial band they meandered with latitudinal displacements of around 1° and Lagrangian periods of 1–2 months. Waves of similar characteristics also have been observed in deep current meter records (Weisberg and Horigan, 1981; Fischer and Schott, 1997; Thierry et al., 1998) and in numerical models (Philander, 1978; Cox, 1980; Böning and Schott, 1993). Böning and Schott found that waves of roughly 1000 km wavelength and 1.5-month period were prominent over nearly the whole zonal extent of the basin. These waves have westward phase velocity and eastward group velocity characteristics of Rossby-gravity (Yanai) waves. They are probably a deep manifestation of instability waves which are generated by the strong shear in the swift near-surface currents (Philander, 1978; Cox, 1980), or by the swift western boundary currents near the equator.

5. Discussion

Several characteristics of the equatorial jets observed by floats have been seen in results of model simulations. Thompson and Kawase (1993) and Li et al. (1996) calculated the net Langrangian circulation using equatorial models and periodic (100–400 d) forcing near the eastern boundary. Li et al. used 365-d period forcing in order to model the observed long Rossby waves and superimposed a 45-d period forcing in order to simulate the observed Yanai waves of that period. In the interior, model floats drifted westward along the equator (approximately 1N–1S) in the Stokes drift of the equatorially trapped long Rossby waves. Model floats drifted eastward between roughly 3N–1N and between 1S and 3S. The meridional structure of the Stokes drift of the model Rossby wave is very similar to the meridional structure of the observed jets (Fig. 12), although the highest modeled eastward flows were located about 1° closer to the equator. The model floats did not follow the mean Eulerian velocity, which was generally opposite to the Stokes drift. The amplitude of the model Lagrangian mean velocity was around 1–2 cm/s near the equator. The Stokes drift was around 4 cm/s near the equator and was partially countered by a weaker Eulerian mean. Thus, the mean velocities of model floats are less than but fairly close to the SOFAR float mean velocities.

In order for these models to be relevant to the observed jets, we would expect to see floats oscillate in direction at the period of the seasonal forcing, and we do. Although the observed seasonal cycle is large at least in the two northern bands, 3N–1N and 1N–1S, the observed seasonal cycle appears to be less pronounced than the modeled

cycle and less pronounced than that measured by current meters near 14W (Thierry et al., 1998). This could be due to the chaotic behavior of floats when waves of several different periods are superimposed as discussed by Li et al. (1996).

Another model result that could be relevant to the equatorial floats is that nonlinearities near the western boundary can create eastward flow that penetrates from the western boundary into the interior along the equator (Thompson and Kawase, 1993; Li et al., 1996). Two floats (5 and 9) did just that during the first six months of the experiment. It also has been suggested that transients in the DWBC are able to generate eastward flow on the equator, which draws out water from the western boundary (Kawase et al., 1992).

5.1. Equatorial CFC plume

CFC-rich water has been traced from its origin in the Labrador Sea (Pickart, 1992) southward in the DWBC and across the equator near a depth of 1700 m (Weiss et al., 1985, 1989; Fine and Molinari, 1988; Molinari et al., 1992). A near-equatorial plume of CFC-rich water extends near 1700 m from the DWBC in the west across the Atlantic into the Gulf of Guinea. Weiss et al. (1989) estimated that roughly two-thirds of the integrated CFC lies in the equatorial plume and one-third along the western boundary south of the equator. Although some maps of the equatorial plume show it centered at the equator (Weiss et al., 1985, 1989; see Fig. 1 shown by Li et al., 1996), virtually all detailed sections across the equator in the mid-Atlantic reveal that the highest concentration of CFC is centered south of the equator near 2S (Fig. 14, Table 3). The limits of the CFC plume obtained by averaging the limits of the highest CFC contours on five individual sections are 1280–1880 m and 0.2S–3.8S (Table 3).

The only possible exception to the southern location of the plume in the mid-Atlantic was a section made near 25N by Doney and Bullister (1992). This section shows the CFC-11 plume to be roughly centered near the equator (3S–3N), but the two most southern stations near 1S and 3S leave a gap at 2S, and the bottle spacing is very sparse at 3S. It seems entirely possible that the maximum in CFC-11 could have been south of the equator but unsampled by the section. Doney and Bullister show the contour of maximum CFC-12 open to the south of 3S, implying that they only sampled the northern part of the CFC maximum. The only documented anomaly from the location of the plume south of the equator is from a SAVE section (Table 3) at 0.5W, which shows the CFC maximum between 2N and 4N next to the northern boundary of the Gulf of Guinea (Weiss et al., 1989; personal communication).

The apparent eastward velocity of the CFC-rich water near the equator was estimated three ways by Andrié et al. (1998). The time lag from the apparent ages of the plume at 35W and 4W gave a mean velocity of 1.5 cm/s. The eastward progression of the CFC-rich water between 1985 (TTO) and 1993 (CITHER) gave a mean eastward velocity of 1.4 cm/s. The F-11/F-12 age at 4W implied that the water had traveled from the Labrador Sea to 4W at a mean velocity of 1.9 cm/s. These estimates agree with the earlier estimates of apparent eastward velocity of 2 cm/s by Weiss et al. (1989).

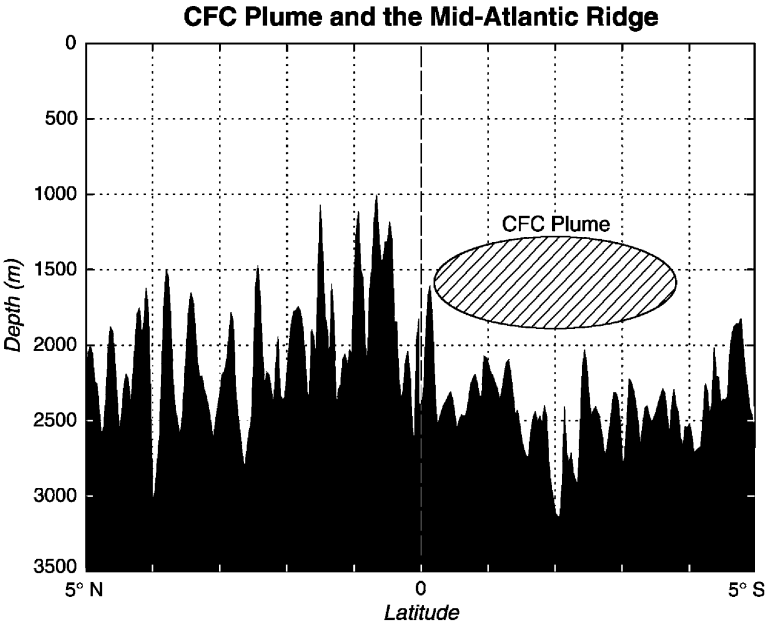

Fig. 14. The CFC plume in the mid-Atlantic is centered south of the equator near 2S. The limits of the plume shown here are averages of the highest CFC concentrations observed on five sections across the equator between 28W and 4W (Table 3). The seafloor depth profile shows the crest of the mid-Atlantic Ridge. The highest elevation at each latitude was obtained from ETOPO2 data (Smith and Sandwell, 1997) courtesy of Roger Goldsmith. The Ridge is roughly 500 m lower south of the equator under the plume than north of the equator. The ridge crest north of the equator is centered near 31W and is west of the sections listed in Table 3. The ridge crest south of the equator is centered near 12W and is east of all sections except those at 4W and 0.5W.

It is striking how well the location of the CFC-rich plume south of the equator matches the location of the southern eastward jet observed by our SOFAR floats. The close match suggests that the plume was advected eastward by the jet. The 4.9 cm/s mean velocity of the jet is somewhat faster than the apparent eastward propagation rate of the CFC plume, but this difference could be caused by the exchange of water between the southern jet and the other jets in the equatorial band as observed by floats. The apparent mean eastward velocity estimated from the CFC data could be less than the mean velocity of the jet because recirculations and turbulent mixing with surrounding water tend to slow the along-jet apparent spreading rate of CFC. This is similar to why the apparent mean velocity of the DWBC from CFC data is less than the mean velocity of the DWBC as measured by current meters and floats (unless one includes the recirculations and equatorial diversions in the estimates). Presumably, parcels of CFC-rich water are advected by the currents like the floats are. Therefore the float trajectories show how the CFC-rich water moves in the equatorial region.

Table 3
Observations of equatorial CFC plume

Date	Long	Peak CFC Lat	Width Lat	Depth (m)	Reference	Comments
1983	28W	4S	1S–5S	1300–1800	Weiss et al. (1989, 1991) and personal comm.	TTO–TAS
1988	25W	?	3N–?	1200–2100	Doney and Bullister (1992)	OC202
1993	25W	1.5S	1N–4S	1000–1900	Doney et al. (1998)	NA93
1987–88	17W	3S	0–6S	1300–1900	Weiss et al. (1989) and personal comm.	SAVE
1987–88	4W	1S	0–2S	1500–2000	Weiss et al. (1989) and personal comm.	SAVE
1993	4W	1.5S	1S–2S	1400–1600	Andrié et al. (1998)	CITHER
1987–88	0.5W	4N	2N–4N	1500–1800	Weiss et al. (1989) and personal comm.	SAVE

Notes: The width and depth of the plume listed here represent the limits of the highest contour of CFC-11 or CFC-12 shown on the sections and are a general indication of the high CFC core. TTO–TAS is the Transient Tracers in the Ocean Tropical Atlantic Study. SAVE is the South Atlantic Ventilation Experiment. CITHER is the Circulation Thermohaline Experiment. OC202 is R/V *Oceanus* cruise 202. The NA93 section was made on R/V *Malcolm Baldrige* cruise 93-13. The 1983 AJAX section near 4W found no measurable CFC at the depth and latitude where the CFC plume was found later in 1987–88 and 1993 (Weiss, personal communication). On both the 25W sections in 1988 and 1993 a CFC-rich core was also observed near 3800 m and 2S in the lower North Atlantic Deep Water.

The overall thickness and width of the CFC plume are significantly larger than the region of highest CFC concentration (Fig. 14). For example, at 25W the CFC plume extended in depth from 1000 to 2600 m and in latitude from 6N to at least 5S, the southern extent of the section (Doney et al., 1998). This shows that the three floats that drifted the farthest eastward near 2S were in the CFC plume. Float 24 which started near a depth of 1125 m, drifted eastward, and gradually descended in the upper part of the plume. Float 1, which started near 1825 m, drifted fast eastward in the central region of the plume and gradually descended below the highest CFC concentrations. Float 203, at a nearly constant depth of 2500 m (Hogg and Owens, 1998) drifted eastward in the lower part of the plume.

The two sections in the mid-Atlantic near 25W (Doney and Bullister, 1992; Doney et al., 1998) also measured a deeper CFC-rich core centered near 3800 m and 2S in lower North Atlantic Deep Water. This deep core lies adjacent to the southern flank of the mid-Atlantic Ridge. The vertical stacking of the two CFC cores implies that the southern jet would have extended down to the lower core and could have advected it eastward.

If there are northern and southern jets as the floats suggest, then why does the CFC plume coincide with only the southern jet? There are several possible explanations for this. First is that the southern jet could be faster than the northern jet. Although the

southern jet average velocity (Table 2) is somewhat faster than that of the northern jet and therefore could dominate the advection of the plume, the data are so sparse that we cannot be certain this is a correct explanation. When averaged by method 2 (Table 2) the velocities of the northern and southern jets are similar.

The second explanation is that the northward recirculation of DWBC water in the region north of the equatorial band and west of the mid-Atlantic Ridge (Fig. 9; Molinari et al., 1992; Friedrichs and Hall, 1993; McCartney, 1993) could advect CFC-rich water away from the northern jet depriving it of a CFC-rich source. The best evidence for a recirculation from floats comes from float 14, which drifted fast down the western boundary in the DWBC to the equator and then recirculated back northwestward again to around 8N. For five months (August 1989 to January 1990) float 14 drifted eastward in the northern jet from 42W to 35W before peeling off to drift northwestward in the recirculation region. The evidence from this one float is in agreement with the concept of the recirculation limiting the amount of CFC-rich water flowing eastward in the northern jet.

The third explanation is the southeastward direction of the western boundary in the equatorial Atlantic. This results in the 2N line intersecting the western boundary around 800 km farther west than does the 2S line, which means that starting at the western boundary a water parcel would need to drift 800 km farther along 2N to reach the same longitude than along 2S. At 2N the DWBC appears to be tightly constrained against the western boundary, but at 2S the DWBC appears to be diverted eastward by a line of seamounts extending eastward near 4S. The seamounts appear to help initiate the southern jet that begins near the boundary where CFC-rich water is found. Float 1 clearly demonstrates how water lying only 100 km from the boundary can be advected directly away from the boundary in the southern jet and carried long distances eastward.

The fourth explanation involves the configuration of the mid-Atlantic Ridge, which is much shallower north of the equator than south of it (Fig. 14). Near 2N the Ridge crest rises up to 1500 m in several places, which could cause a much larger disruption or partial blocking of a CFC plume than near 2S where the Ridge crest lies below 2000 m. It looks much easier for a plume to cross the Ridge near 2S than near 2N (Fig. 14). In addition the 2N line crosses the mid-Atlantic Ridge near 31W about 2100 km farther west than where the 2N line crosses the Ridge near 12W. This is due to the large $\sim 20^{\circ}$ eastward displacement of the Ridge near the equator. In this mid-Atlantic region (31W–12W) the southern jet and the CFC plume lie south of the mid-Atlantic Ridge crest. If the Ridge causes some disruption or blocking of the jets and an enhanced exchange between jets as implied by the float trajectories, then the southern jet would remain undisrupted much farther east (2100 km) than would the northern jet. The mid-Atlantic sections across the equator listed in Table 3 at 28W, 25W, and 17W all lie *east* of the Ridge at 2N but *west* of the Ridge at 2S. Therefore, the asymmetry of the CFC plume with respect to the jets is possibly a result of the eastward offset of the Ridge in the vicinity of the equator. The Ridge could have disrupted or blocked a CFC plume near 2N before it reached the sections.

To conclude this discussion, several possible reasons were suggested to explain why the southern jet appears to advect the CFC-rich plume eastward but the northern jet

does not do so – a possibly faster speed of the southern jet, the northwestward recirculation of the CFC-rich water north of the equator and west of the Ridge, the shape of the western boundary that seems to directly feed CFC-rich water into the southern jet, and the shape of the mid-Atlantic Ridge, which could cause a larger disruption of the northern jet than the southern jet. Given the rather limited SOFAR float observations it is difficult to know which of these explanations are most relevant.

6. Summary

At times the DWBC flows directly southward across the equator with a mean velocity of 8–9 cm/s averaged over long distances ($\sim$2800 km). Some DWBC water recirculates near the boundary, which reduces its mean along-boundary velocity to around 1 cm/s. At other times DWBC water is diverted eastward near the equator for long periods of time – 1.7 yr for float 6, 3.3 yr for float 9 – which also can reduce the mean along-boundary velocity to 1–2 cm/s. These mean velocities are considerably smaller than instantaneous along-boundary float velocities, which can exceed 50 cm/s and smaller than mean along-boundary values, which are around 20 cm/s in the DWBC (Fig. 9). The SOFAR float trajectories demonstrate why the apparent mean velocity of the CFC plume is less than the observed mean velocity of the DWBC jet.

The 1800 m float trajectories revealed mean eastward flowing jets centered at 2S and 2N bounding a mean westward flow on the equator (1S–1N). The equatorial current (1S–1N) was observed to change direction from eastward during the first six months of the experiment to mainly westward for the rest of the experiment. This is in agreement with results from moored current meter records, which document long period fluctuations at the equator (Fischer and Schott, 1997). The eastward jets are around two degrees wide, at least 500 m thick and have mean Lagrangian velocities of 3–5 cm/s averaged over two degrees in latitude. The jets appeared to fluctuate or pulse seasonally. The southern jet coincides with a plume of CFC-rich water that extends near 2S across the Atlantic into the Gulf of Guinea. The CFC plume is interpreted to have been advected eastward by the southern jet and to have been gradually mixed within the equatorial band by exchanges among the series of zonal jets as observed by the floats. Several possible reasons were suggested to explain why a CFC-rich plume does not coincide with the northern jet in the mid-Atlantic. These include the recirculation located north of the equator and west of the Ridge which carries CFC-rich water away from the northern jet, the shape of the western boundary which appears to preferentially feed CFC-rich water into the southern jet, and the height and equatorial offset of the mid-Atlantic Ridge, which is a more formidable obstacle to the northern jet than to the southern jet.

Acknowledgements

Contribution number 9570 from the Woods Hole Oceanographic Institution. Funds were provided by National Science Foundation grants OCE85-21082,

OCE85-17375, and OCE91-14656. J.R. Valdes, R. Tavares, B. Guest and G. Tupper were in charge of the SOFAR floats and listening stations which were launched from the RV *Oceanus* and RV *Iselin*. C. Wooding and M. Zemanovic tracked the floats, generated figures, and calculated statistics. M.A. Lucas typed the manuscript. J. Doucette created some of the graphics. A draft of this paper was written while PLR visited the Discovery Bay Marine Laboratory in Jamaica. Michael Haley and others at the Marine Lab helped make the visit a pleasant and productive one. This paper is dedicated with fond memories to Gerold Siedler, our long-time colleague on the other side of the Atlantic.

References

Andrié, C., Ternon, J.-F., Messias, M.J., Memery, L., Bourles, B., 1998. Chlorofluoromethane distributions in the deep equatorial Atlantic during January–March 1993. Deep-Sea Research, in press.

Böning, C.W., Schott, F.A., 1993. Deep currents and the eastward salinity tongue in the equatorial Atlantic: Results from an eddy-resolving, primitive equation model. Journal of Geophysical Research 98, 6991–6999.

Broecker, W., 1991. The great ocean conveyor. Oceanography 4, 79–89.

Colin, C., Bourlès, B., Chuchla, R., Dangu, F., 1994. Western boundary current variability of French Guiana from moored current measurements. Oceanologica Acta 17, 345–354.

Cox, M.D., 1980. Generation and propagation of 30-day waves in a numerical model of the Pacific. Journal of Physical Oceanography 10, 1168–1186.

Didden, N., Schott, F., 1993. Eddies in the North Brazil Current retroflection region observed by Geosat altimetry. Journal of Geophysical Research 98, 20 121–20 131.

Doney, S.C., Bullister, J.L., Wanninkhof, R., 1998. Climatic variability in upper ocean ventilation diagnosed using chlorofluorocarbons. Geophysical Research Letters, in press.

Doney, S.C., Bullister, J.L., 1992. A chlorofluorocarbon section in the eastern North Atlantic. Deep-Sea Research 39, 1857–1883.

Doney, S.C., Jenkins, W.J., 1994. Ventilation of the deep western boundary current and abyssal western North Atlantic: estimates from tritium and ^{3}He distributions. Journal of Physical Oceanography 24, 638–659.

Fine, R.A., Molinari, R.L., 1988. A continuous deep western boundary current between Abaco (26.5°N) and Barbados (13°N). Deep-Sea Research 35, 1441–1450.

Fischer, J., Schott, F.A., 1997. Seasonal transport variability of the deep western boundary current in the equatorial Atlantic. Journal of Geophysical Research 102, 27 751–27 769.

Fratantoni, D.M., Johns, W.E., Townsend, T.L., 1995. Rings of the North Brazil Current: Their structure and behavior inferred from observations and a numerical simulation. Journal of Geophysical Research 100, 10 633–10 654.

Friedrichs, M.A.M., Hall, M.M., 1993. Deep circulation in the tropical North Atlantic. Journal of Marine Research 51, 697–736.

Gouriou, Y., Bourlès, B., Mercier, H., Chuchla, R. Deep jets in the equatorial Atlantic Basin. Journal of Geophysical Research, submitted.

Hall, M.M., McCartney, M.S., Whitehead, J.A., 1997. Antarctic bottom water flux in the equatorial western Atlantic. Journal of Physical Oceanography, 27, 1903–1926.

Hogg, N.G., Owens, W.B., 1999. Direct measurement of the deep circulation within the Brazil Basin. Deep-Sea Research II 46, 335–353.

Johns, W.E., Fratantoni, D.M., Zantopp, R.J., 1993. Deep western boundary current variability off northeastern Brazil. Deep-Sea Research 40, 293–310.

Johns, W.E., Lee, T.N., Schott, F., Zantopp, R.J., Evans, R.H., 1990. The North Brazil Current retroflection: seasonal structure and eddy variability. Journal of Geophysical Research 95, 22 103–22 120.

Kawase, M., Rothstein, L.H., Springer, S.R., 1992. Encounter of the deep western boundary current with the equator: a numerical spin-up experiment. Journal of Geophysical Research 97, 5447–5463.

Li, X., Chang, P., Pacanowski, R.C., 1996. A wave-induced stirring mechanism in the mid-depth equatorial ocean. Journal of Marine Research 54, 487–520.

McCartney, M.S., 1993. Crossing of the equator by the deep western boundary current in the western Atlantic Ocean. Journal of Physical Oceanography 23, 1953–1974.

Molinari, R.L., Fine, R.A., Johns, E., 1992. The deep western boundary current in the tropical North Atlantic Ocean. Deep-Sea Research 39, 1967–1984.

Ollitrault, M., 1998. The AAIW general circulation in the Brazil Basin and equatorial Atlantic. Annales Geophysical, Part II: Hydrology, Oceans and Atmospheres 16 (Suppl 11), abstract, p. C543.

Philander, S.G.H., 1978. Forced oceanic waves. Reviews of Geophysics and Space Physics 16, 15–46.

Philander, S.G.H., Hurlin, W.J., Pacanowski, R.C., 1986. Properties of long equatorial waves in models of the seasonal cycle in the tropical Atlantic and Pacific Oceans. Journal of Geophysical Research 91, 14 207–14 211.

Pickart, R.S., 1992. Water mass components of the North Atlantic Deep Western Boundary Current. Deep-Sea Research 39, 1553–1572.

Pickart, R.S., Hogg, N.G., Smethie, W.M., 1989. Determining the strength of the deep western boundary current using the chlorofluoromethane ratio. Journal of Physical Oceanography 19, 940–951.

Ponte, R.M., Luyten, J., Richardson, P.L., 1990. Equatorial deep jets in the Atlantic Ocean. Deep-Sea Research 37(4), 711–713.

Rhein, M., 1994. The deep western boundary current: Tracers and velocities. Deep-Sea Research 41, 263–281.

Rhein, M., Stramma, L., Send, U., 1995. The Atlantic western boundary current: Water masses and transport near the equator. Journal of Geophysical Research 100, 2441–2457.

Richardson, P.L., Zemanovic, M.E., Wooding, C.M., Schmitz Jr. W.J., Price, J.F., 1992. SOFAR float trajectories from an experiment to measure the Atlantic cross equatorial flow (1989–1990). Woods Hole Oceanographic Institution Technical Report WHOI-92-33, 187pp.

Richardson, P.L., Schmitz Jr. W.J., 1993. Deep cross-equatorial flow in the Atlantic measured with SOFAR floats. Journal of Geophysical Research 98(C5), 8371–8387.

Richardson, P.L., Hufford, G., Limeburner, R., Brown, W.S., 1994a. North Brazil current retroflection eddies. Journal of Geophysical Research 99(C3), 5081–5093.

Richardson, P.L., Zemanovic, M.E., Wooding, C.M., Schmitz Jr. WJ., 1994b. SOFAR float trajectories in the Tropical Atlantic 1989–1992. Woods Hole Oceanographic Institution Technical Report WHOI-94-33, 185pp.

Schmitz, Jr. W.J., Richardson, P.L., 1991. On the sources of the Florida Current. Deep-Sea Research 38 (Suppl. 1), S379–S409.

Schott, F., Fischer, J., Reppin, J., Send, U., 1993. On mean and seasonal currents and transports at the western boundary of the equatorial Atlantic. Journal of Geophysical Research 98, 14 353–14 368.

Smith, W.H.F., Sandwell, D.T., 1997. Global sea floor topography from satellite altimetry and ship depth soundings. Science 277, 1956–1962.

Thierry, V., Mercier, H., Treguier, A.M., 1998. Direct observations of low frequency fluctuations in the deep equatorial Altantic. Annales Geophysical, Part II: Hydrology, Oceans and Atmospheres 16 (Suppl. 11), abstract, p. C568.

Thompson, L., Kawase, W., 1993. The nonlinear response of the equatorial ocean to oscillatory forcing. Journal of Marine Research 51, 467–496.

Uchupi, E., 1971. Bathymetric atlas of the Atlantic, Caribbean, and Gulf of Mexico. Woods Hole Oceanographic Institution Technical Report WHOI-71-72, 10 pp.

Weisberg, R.H., Horigan, A.M., 1981. Low-frequency variability in the equatorial Atlantic. Journal of Physical Oceanography 11, 913–920.

Weiss, R.F., Bullister, J.L., Gammon, R.H., Warner, M.J., 1985. Atmospheric chlorofluoromethanes in the deep equatorial Atlantic. Nature 314, 608–610.

Weiss, R.F., Bullister, J.L., Van Woy, F.A., Warner, M.J., Salameh, P.K., Gammon, R.H., 1991. Transient Tracers in the Ocean, Tropical Atlantic Study: Chlorofluorocarbon measurements. Scripps Institution of Oceanography Reference 91-1, January 1991. Scripps Institution of Oceanography, La Jolla, CA 92093-0220, USA.

Weiss, R.F., Warner, M.J., Harrison, K.G., Smethie, W.M., 1989. Deep equatorial Atlantic chlorofluorocarbon distributions. EOS Transactions of the American Geophysical Union 70, 1132.